J Mater Sci (2010) 45:2456–2465
DOI 10.1007/s10853-010-4217-x

Effect of annealing on aqueous stability and elastic modulus of electrospun poly(vinyl alcohol) fibers

Kenneth Kar Ho Wong · Martin Zinke-Allmang · Wankei Wan

Received: 22 August 2009 / Accepted: 9 January 2010 / Published online: 26 January 2010

Abstract Electrospun poly(vinyl alcohol) (PVA) fibers rapidly dissolve in water. Their aqueous stability can be improved by annealing using a combination of controlled temperature and treatment time. The increase in aqueous stability of the PVA fibers is associated with an increase in PVA crystallinity and is defined by X-ray diffraction and the ratio of the Fourier transform infrared spectroscopy band intensities at 1141 and 1425 cm^{-1}. A ratio of intensity of these two infrared bands $\geq$2.5 or ~75% and above in the degree of crystallinity as determined by X-ray diffraction indicates fiber stability in water. Annealing treatment also results in an increase in the stiffness of the fibers. At a treatment temperature of 135 °C for 4 h, the elastic modulus of the fiber increased by 80%. This information is useful when these fibers are being considered for applications in an aqueous environment such as membrane filter or tissue scaffold.

Introduction

Electrospinning [1] is a convenient technique to produce three-dimensional non-woven fiber mats consisting of nanometer-sized fibers made from synthetic and natural polymers [2] including proteins and polysaccharides [3]. Applications being considered include wound dressings [4], membranes [5], drug deliveries [6] and scaffolds for tissue regeneration [7]. Electrospun fiber mats display exceptional performance and efficiency in these applications due to their high surface-to-volume ratios and interconnected porous network. Electrospinning has become the method of choice for their fabrication [8, 9]. For tissue engineering applications, the fibrous scaffolds can also be electrospun with controlled alignment to mimic the structure of the natural extracellular matrix [10, 11].

Poly(vinyl alcohol) (PVA) is a hydrophilic polymer with good thermal stability, chemical resistance and biocompatibility [12]. Although PVA is biostable in physiological environments, it readily dissolves in water and means for its stabilization is necessary to realize its potentials in biomedical applications in the fiber form. PVA can be chemically or physically cross-linked using glutaraldehyde [13, 14], radiations [15, 16], and freezing/thawing processes [17] to achieve good aqueous stability for medical device applications such as artificial meniscus [18], heart valves [19] and wound dressings [20]. For electrospun PVA fibers, glutaraldehyde [21, 22] and methanol [23, 24] have been shown as effective post-processing agents to stabilize the fibers in aqueous media, but the morphological features of the electrospun fibers mats are largely lost. In addition, chemical properties are altered due to the reactive interactions with the stabilizing agents. In our previous work, we demonstrated the suitability of ion beam implantation [25] to stabilize PVA fibers from disintegrating in water. Although the changes in the morphological features were minimal, the cost of the treatment for samples in large quantity and size can be prohibitive. Water stable PVA hydrogels have been prepared by a thermal cycling process. Their stability and mechanical properties control have been

---

K. K. H. Wong · M. Zinke-Allmang
Department of Medical Biophysics, The University of Western Ontario, London, ON N6A 5C1, Canada

M. Zinke-Allmang
Department of Physics and Astronomy, The University of Western Ontario, London, ON N6A 3K7, Canada

W. Wan (✉)
Department of Chemical and Biochemical Engineering, Fordham Center for Biomedical Engineering, The University of Western Ontario, London, ON N6A 5B9, Canada
e-mail: wkwan@eng.uwo.ca

attributed to an increase in the polymer crystallinity [26–28]. For macroscopic PVA samples, thermal annealing has been reported to increase the degree of crystallinity without changing its chemical structure [29, 30]. We hypothesize that thermal annealing will lead to an increase in crystallinity of electrospun PVA fibers. This would result in an improvement in their aqueous stability and a concomitant increase in the fiber mechanical properties.

In this study, we report the use of a high-temperature annealing approach to improve the aqueous stability and mechanical properties of PVA fibers prepared by electrospinning. The change in crystallinity of the fibers as a function of annealing condition was determined using Fourier transform infrared spectroscopy (FTIR) and X-ray diffraction (XRD). Mechanical properties of individual PVA fibers prior to and following annealing were determined using an atomic force microscopy (AFM) multi-point bending test and analysis routine developed in our laboratory [31].

Experimental methods

PVA fiber production by electrospinning

The electrospinning solution is prepared by dissolving 11 wt% of PVA ($M_w = 89{,}000$–$98{,}000$ g/mol, 99+% hydrolyzed, Sigma–Aldrich) in a solvent consisting of 90% de-ionized water and 10% ethanol. Process parameters included an electric field gradient of 1 kV/cm and a solution feed rate of 0.1 mL/h.

For the study of fiber morphology and crystallinity, PVA fibers were collected on a silicon substrate in the form of a randomly orientated non-woven mat. To collect individual, isolated electrospun fibers for AFM mechanical testing, a transmission electron microscopy (TEM) grid (Structure Probe, Inc.) with a 7.5 μm square mesh was used on a silicon substrate and mounted at the center of the collector.

Annealing treatment

The annealing treatment was conducted in a vacuum oven at six different annealing temperatures: 85, 110, 135, 160, 185 and 210 °C. The pressure was maintained at 10 Torr over various lengths of annealing time as stated in later sections. The samples remained in vacuum for further 2 h to cool down before unloading from the oven.

Physical characterization of PVA fibers

The dimension of the fibers for aqueous stability tests and AFM mechanical measurements were determined from SEM topological images, which were obtained with a Leo 1530 (LEO Electron Microscopy Ltd.) at 1 kV, using the Java-based image processing program, ImageJ (National Institutes of Health). No conductive coating was applied to the samples.

The glass transition temperature and the melting temperature of as-spun PVA fibers were determined using differential scanning calorimetry (DSC) (Perkin Elmar Pyris 1). The experiment was performed between 50 and 250 °C at a heating rate of 10 °C per minute. The as-spun fiber has a glass transition temperature of 91.2 °C which is close to the lowest thermal treatment temperature we used. The melting temperature is a function of annealing temperature and varies from a low of 227.7 °C for the as spun fibers to a high of 232.5 °C after annealing at 135 and 160 °C.

Attenuated total reflectance Fourier transform infrared spectroscopy (ATR-FTIR) was used to qualitatively verify the increase in the degree of crystallinity of the PVA sample upon heat treatment. In the present experiments, an FTIR spectrometer (Bruker Vector 22; Milton, ON) with a horizontal attenuated total reflectance attachment and a diamond crystal. The chamber was continuously purged with dry air to reduce water vapor and carbon dioxide content. The background spectrum was collected prior to that of the PVA fiber samples.

X-ray diffraction (XRD) spectra were collected using a Rigaku-Rotaflex RU-200BH diffractometer with a Co-K_α radiation (wavelength $\lambda = 1.79$ Å) source operating at 30 kV and 44 mA. The 2θ spectra were scanned from 16.0° to 32.0° with a 0.1° step size. The diffraction peak (FWHM) were analyzed by fitting the Pearson VII function [32]. The average crystallite size (P) was estimated by using the Scherrer's equation [33]:

$$P = \frac{k\lambda}{(w\cos\theta)} \quad (1)$$

where w is again FWHM in radians, θ is the Bragg's angle, and $k = 1$ (or 0.9) is a constant and related to several aspects including the shape of the crystal and the Miller index of the reflecting crystallographic planes and crystallite shape. The degree of crystallinity (X_c) was determined from the ratios of the areas under the crystalline peaks and the respective halos using the method of Hermans and Weidinger [34, 35]:

$$X_c = \frac{A_c}{(A_c + A_a)} \quad (2)$$

where A_c and A_a are the area of crystalline and amorphous (halo) region, respectively.

Aqueous stability tests

The annealed PVA fibers were immersed in de-ionized (DI) water for 1, 10 and 30 days at room temperature. The samples were then transferred into isopropyl alcohol for 5 min before loading in a chamber to complete the drying process under vacuum (10 Torr) for later SEM characterization.

Mechanical measurements using AFM

Mechanical testing of individual PVA fibers was performed using a multimode AFM with a Nanoscope IIIa controller (Veeco Instruments) at room temperature with relative humidity of ≤9% (nitrogen gas ambient). Two different triangular silicon nitride cantilevers (NP Series Probes, Veeco Instruments) with nominal spring constants of 0.58 and 0.32 N/m, respectively, were chosen to carry out the mechanical testing of the fibers before and after annealing. The actual spring constants were determined using the thermal noise technique [36] which yielded $k_1 = 0.31 \pm 0.01$ N/m and $k_2 = 0.24 \pm 0.01$ N/m, respectively.

A multi-points bending test was performed on 16 fibers in the AFM force–volume mode, as described previously [25], both before and after annealing. The force spectra with the z-scan size limited at 500 nm were acquired for positions in an array of 64 × 64 pixels spanning square regions of width 3.5–5.0 μm at a z-scan rate of 5 Hz. Three threshold levels of 100, 125 and 150 nm were used throughout this study.

The diameter of each fiber was determined by averaging measurements at 10 locations along the suspended portion of the fiber based on high-resolution SEM images. The uncertainties are due to diameter irregularities of the fiber.

Data was extracted from the force–volume images and analyzed using the Igor Pro software package (Wavemetrics) with a custom analysis routine based on a clamped-beam model, as described previously [25].

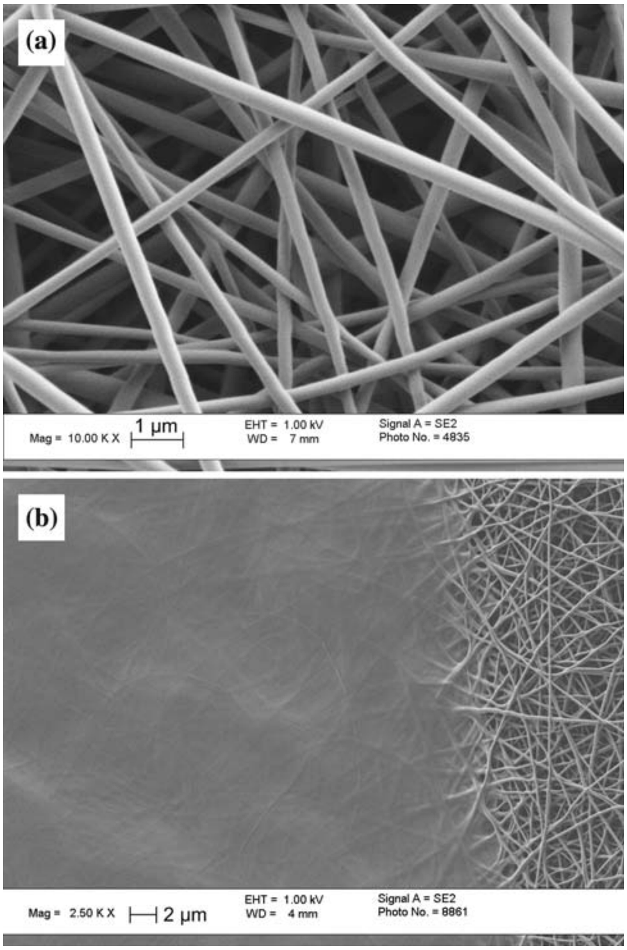

Fig. 1 SEM images of original PVA fibers **a** in high magnification and **b** after immersed in DI water for 1 min (area affected at the *left side*)

Results and discussion

Effect of annealing treatment on fiber stability in water–temperature dependence

Figure 1a shows an SEM image of randomly orientated, non-woven PVA fibers prepared by electrospinning before annealing. The as-spun PVA fibers display very poor stability in water as shown on the left side of a low magnification SEM image (Fig. 1b). After immersed in DI water for 1 min, the fiber structure has completely disappeared and a film with no porosity was formed. To investigate the enhancement of aqueous stability of PVA fibers by annealing, four samples with average fiber diameter in the range of 244 to 270 nm were treated separately at 85, 110, 135 and 160 °C for 4 h each. SEM images of these fibers after annealing at these temperatures are shown in Figs. 2a, 3a, 4a, and 5a, respectively. In all cases, the fibers showed no significant morphological and size (diameter) changes after treatment. These samples were then immersed in DI water for 1 day and re-examined with SEM. The results are shown in Figs. 2b, 3b, 4b, and 5b. The sample treated at 85 °C and shown in Fig. 2b was partially dissolved, leading to a reduction in fiber diameter and porosity of the fibrous structures. Annealing at 110 °C also resulted in partial dissolution; however, in this case, the aqueous instability led to fusion of some of the fibers into bundles. As a result, they are no longer cylindrical and a slight reduction in the average diameter was observed (Fig. 3b). The porosity of the woven structure was also reduced. Figures 4b and 5b show the SEM images of the samples treated at 135 and 160 °C, respectively, after immersion in DI water for 1 day. The morphology and average fiber diameter of these two samples remained unchanged, indicating good aqueous stability. To investigate the longer term stability, all annealed samples were re-immersed in DI water for an additional 10 and 30 days. The results are summarized in Figs. 2c, 3c, 4c, and 5c and Figs. 2d, 3d, 4d,

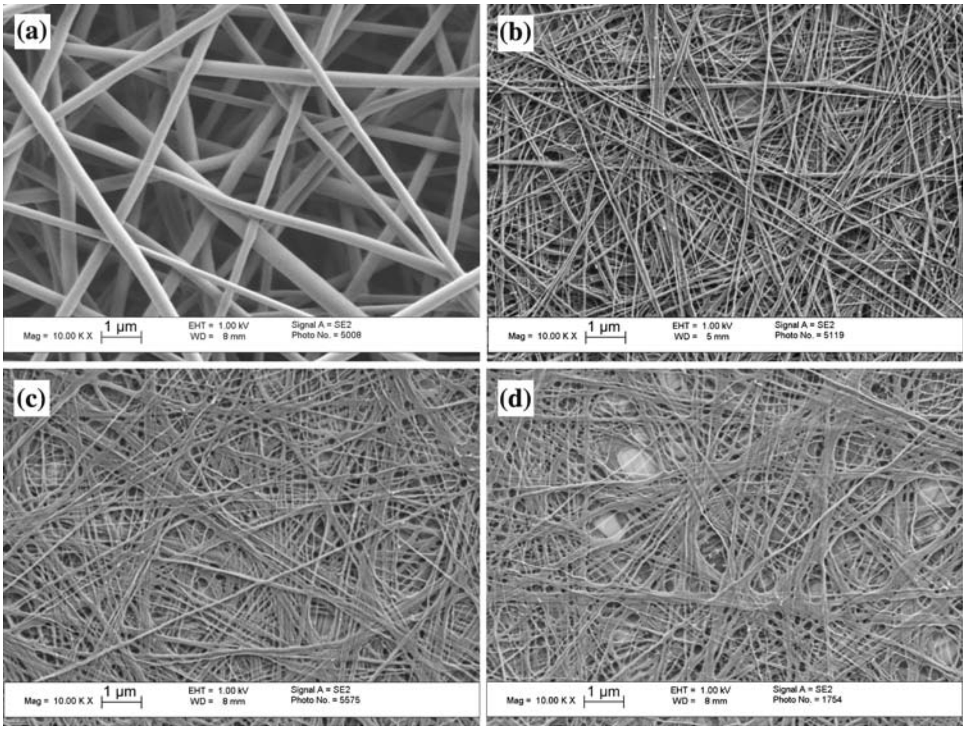

Fig. 2 SEM images of PVA fibers with 4 h of 85 °C annealing treatment after **a** annealing, **b** immersed in DI water for 1 day, **c** immersed in DI water for 10 days, and **d** immersed in DI water for 30 days

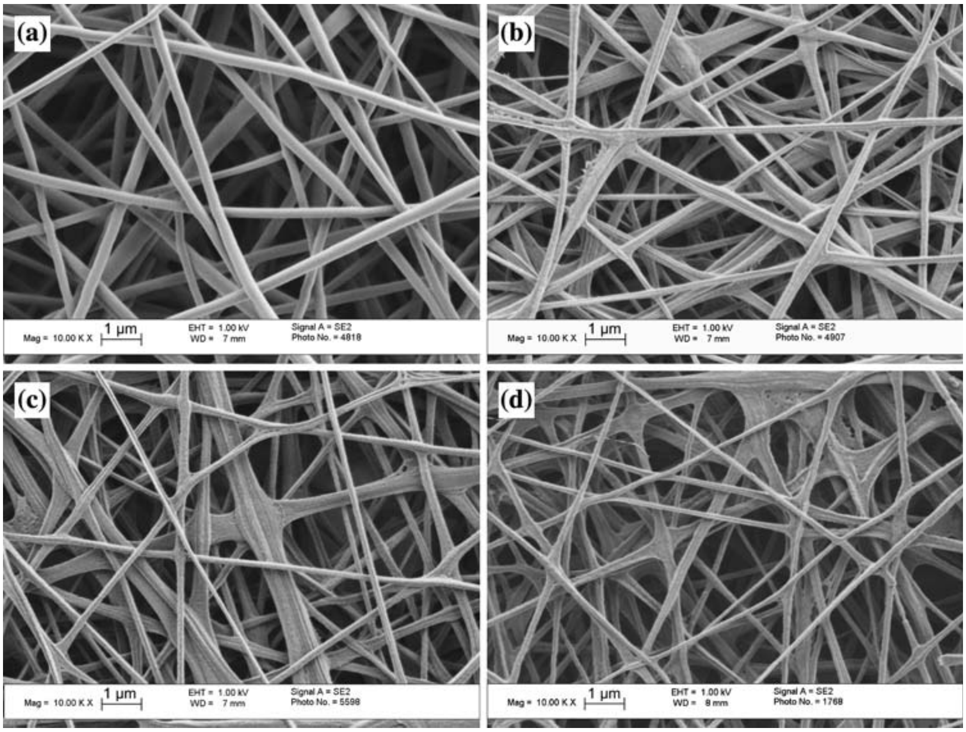

Fig. 3 SEM images of PVA fibers with 4 h of 110 °C annealing treatment after **a** annealing, **b** immersed in DI water for 1 day, **c** immersed in DI water for 10 days, and **d** immersed in DI water for 30 days

and 5d, respectively. It can be seen that these results are similar to those shown in Figs. 2b, 3b, 4b, and 5b after immersed in DI water for 1 day, indicating no significant dissolution after day 1.

To quantify the aqueous stability of these fibers under the four different annealing conditions, the average fiber diameters (determined from 250 randomly selected fibers) of samples corresponding to Figs. 2a–d, 3a–d, 4a–d and 5a–d were determined and are summarized in Fig. 6. Heat treatment at 85 °C resulted in a significant reduction in average fiber diameter from 270 ± 60 nm to 46 ± 14 nm (the uncertainties are standard deviation (SD)) after 1 day

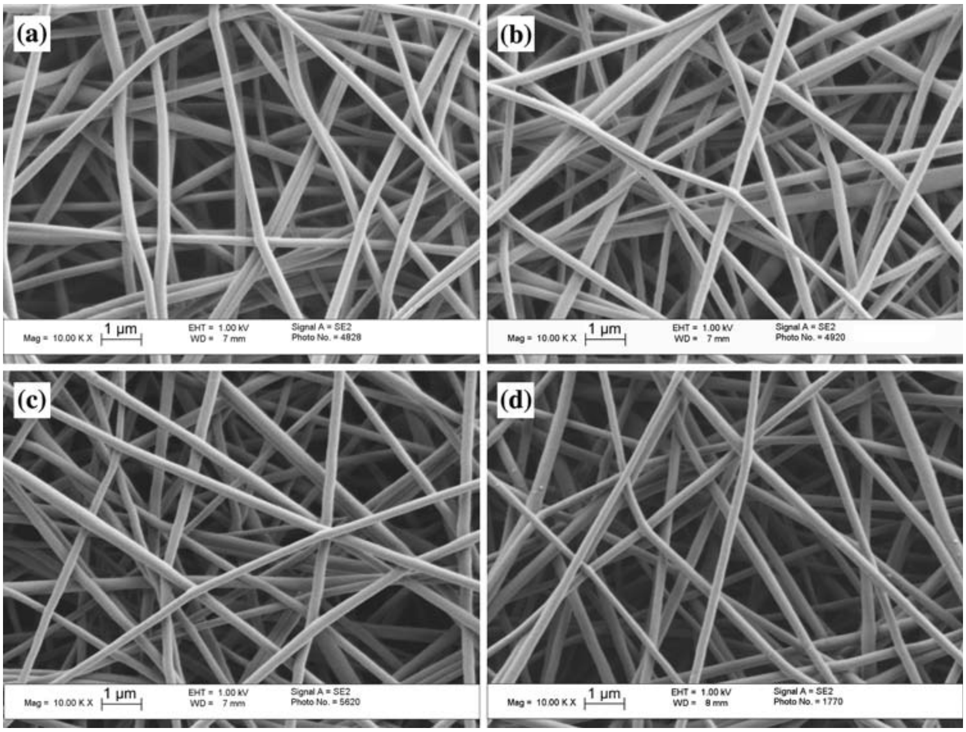

Fig. 4 SEM images of PVA fibers with 4 h of 135 °C annealing treatment after **a** annealing, **b** immersed in DI water for 1 day, **c** immersed in DI water for 10 days, and **d** immersed in DI water for 30 days

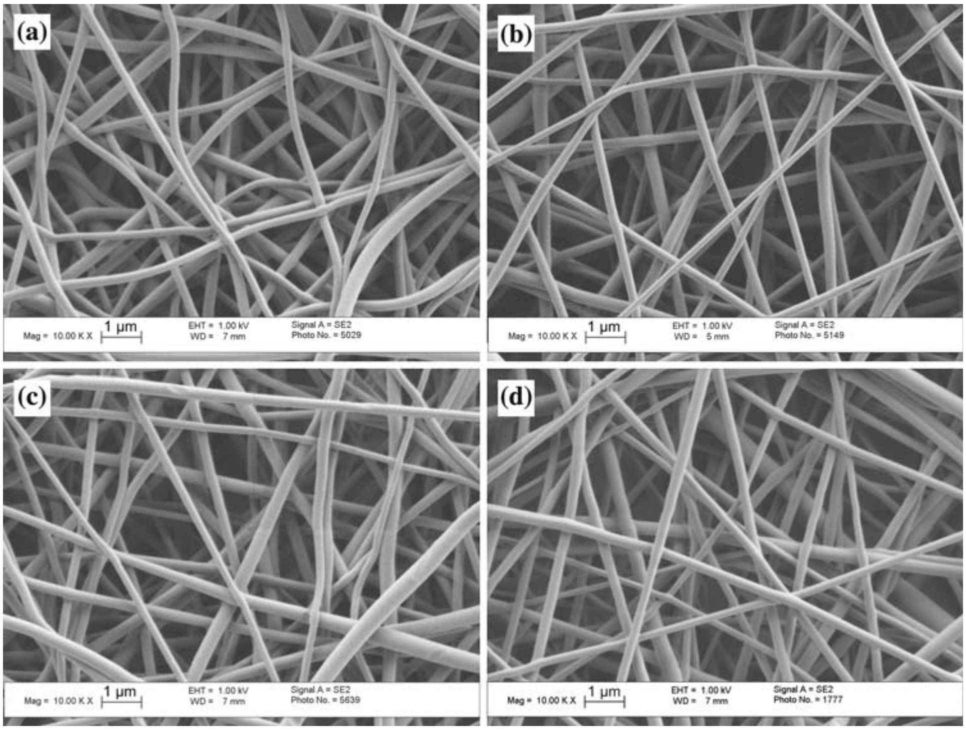

Fig. 5 SEM images of PVA fibers with 4 h of 160 °C annealing treatment after **a** annealing, **b** immersed in DI water for 1 day, **c** immersed in DI water for 10 days, and **d** immersed in DI water for 30 day

in DI water and remained unchanged after 10 days. Treatment at 110 °C led to a lower degree of fiber size reduction after 1 day in DI water. The average fiber diameter decreased by 34% to 190 ± 50 nm. However, the average fiber diameter increased from 190 to 220 nm after immersed in DI water for 10 days. This increase is due to the bundling of some of the individual fibers as shown in Fig. 3c. Contrast to these results, fibers treated at 135 and 160 °C were stable after immersed in DI water for up to 30 days. Both the morphology and average fiber diameter remained unchanged. These 30 days stability test results provide sufficient confidence to allow for extrapolation of

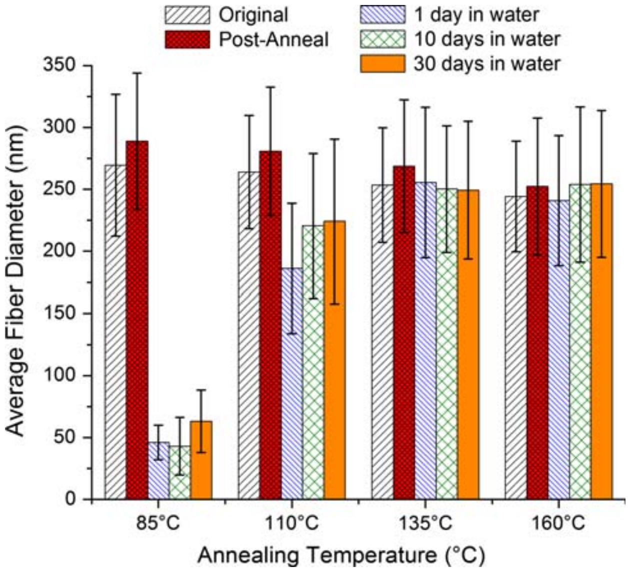

Fig. 6 Fiber diameters after 4 h of annealing at four different temperatures; at five different stages during the stability test in DI water (the error bars are standard deviation)

stability of these annealed fibers to significantly longer time points.

The increase in aqueous stability of electrospun PVA fibers can either be a result of chemical, physical or a combination of these changes since it has been established that annealing of bulk PVA does not result in chemical change but in a change in the degree of crystallinity [29, 30]. The most likely explanation of our observations is an increase in fiber crystallinity, although the dimension of the PVA fibers is significantly different from that of bulk PVA. For a given treatment time, there is a threshold temperature above which these fibers become stable in an aqueous solution. This is an important requirement for biomedical and other applications in an aqueous environment. For an annealing time of 4 h, the minimum temperature to obtain stable PVA fibers is ~135°.

Effect of annealing treatment on fiber stability in water–time dependence

The effect of annealing time on fiber stability was investigated at 110 and 135 °C with time varying between 30 min and 8 h. The results are summarized in Fig. 7. The morphology of fibers treated for 8 h at 110 °C is shown in Fig. 7a after immersed in DI water for 10 days, which is a treatment very similar to that for 4 h (Fig. 3c), i.e., the extra 4 h of treatment at this temperature did not further improve the stability of the fibers in DI water.

The results for annealing at 135 °C for 30 min and 1 h are shown in Fig. 7b and c, respectively. From Fig. 7b, it can be seen that even for a short treatment, the fiber stability was much improved and the cylindrical shape of the fibers was largely retained, but some of the fibers stuck together to form bundles. Close examination of their surface at some intersection points (e.g. in Fig. 8) also indicated an increase in surface roughness of the fiber, which is a sign of selective dissolution. This indicates that 30 min

Fig. 7 SEM images of PVA fibers with **a** 8 h of 110 °C, **b** 30 min of 135 °C, and **c** 1 h of 135 °C treatment after immersed in DI water for 10 days

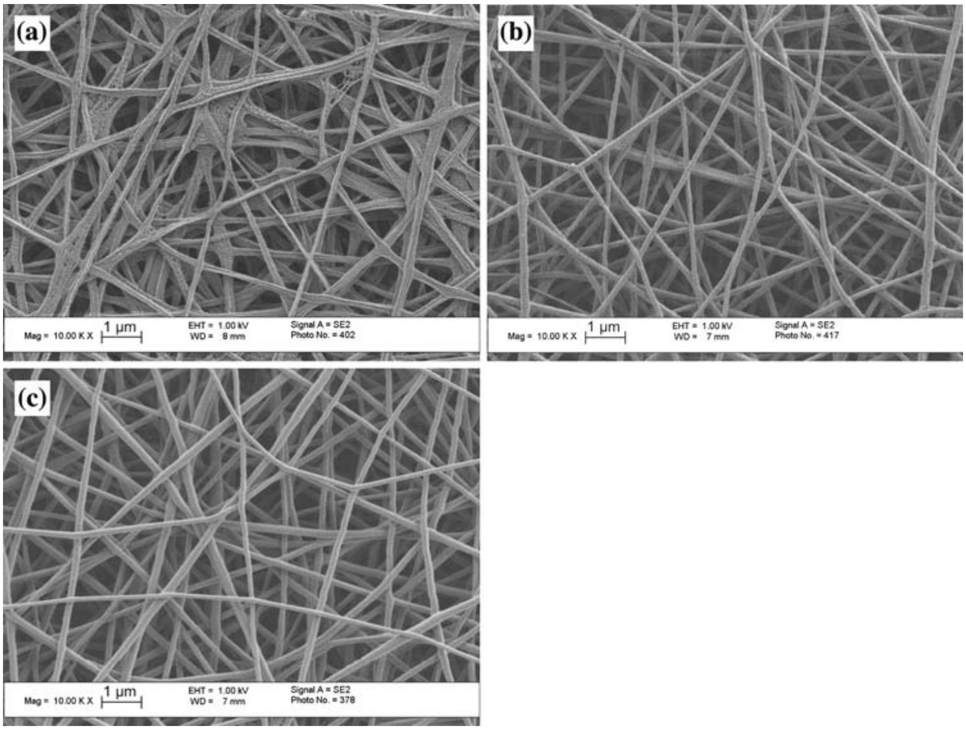

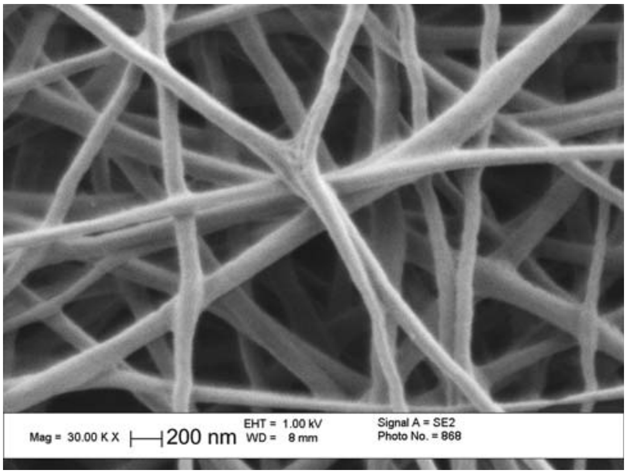

Fig. 8 High-resolution SEM image of the sample shown in Fig. 7b

heat treatment at 135 °C is not enough to establish a sufficient stability of the fibers.

When the treatment time was increased to 1 h, the SEM results shown in Fig. 7c indicate good fiber stability, comparable to those shown in Fig. 4c after 4 h heat treatment. The fibers maintained their smooth surface, similar to that of the as-spun fibers, and did not bundle together. The average fiber diameter also exhibited no change over the entire series of experiments (180 ± 30 nm for as-treated and 175 ± 30 nm after immersed in water for 10 days), indicating that for fiber stability in water, a heat treatment of 1 h at 135 °C is sufficient.

These results are consistent with the assumption that the increase in fiber stability is associated with an increase in fiber crystallinity. A minimum temperature is required to allow polymer chain mobility within the fiber, which is a prerequisite for the creation of sufficient crystallinity. On the other hand, once this temperature is reached, the time required to achieve stability is only a function of the polymer chain mobility.

Effect of thermal treatment on mechanical properties

The change in mechanical properties associated with increased fiber stability in water by heat treatment was also investigated. Sixteen fibers with diameters ranging from 150 to 250 nm were analyzed using the AFM-based bending test before annealing. This yielded a mean elastic modulus of 4.4 ± 1.4 GPa (the uncertainties are SD). These fibers were then annealed for 4 h at 135 °C. During annealing the fiber diameter range decreased to 135–230 nm which corresponded to a diameter reduction of about 10% for each fiber. A bending test using the AFM was again used to determine the elastic modulus of these 16 fibers after annealing. The results showed a significant increase in the elastic modulus of all fibers to a mean value of 7.6 ± 2.3 GPa. This is an increase of 80% over the fibers before treatment. The summarized results are provided in Table 1. The treated fibers do not possess an anisotropic core–shell structure as the AFM force–volume

Table 1 The dimensional and elastic modulus changes of individual fibers before and after 4 h of 135 °C annealing

Fiber #	Pre-annealing			Post-annealing		
	Length (μm)	Diameter (nm)	Elastic modulus (GPa)	Length (μm)	Diameter (nm)	Elastic modulus (GPa)
1	3.6	252 ± 7	2.7 ± 0.6	3.6	232 ± 7	4.1 ± 0.7
2	3.4	183 ± 3	4.5 ± 0.6	3.2	164 ± 4	6.3 ± 0.6
3	4.5	199 ± 4	4.1 ± 0.6	4.5	182 ± 3	7.9 ± 0.9
4	3.7	207 ± 5	2.7 ± 0.3	3.7	179 ± 3	7.3 ± 0.9
5	3.5	181 ± 3	6.1 ± 0.8	3.5	161 ± 3	8.6 ± 1.1
6	3.3	191 ± 2	5.7 ± 0.7	3.2	178 ± 2	8.4 ± 1.0
7	3.8	238 ± 5	2.6 ± 0.3	3.9	217 ± 3	5.8 ± 0.9
8	4.7	153 ± 2	6.3 ± 0.7	4.6	135 ± 3	8.5 ± 0.9
9	4.2	242 ± 3	4.0 ± 0.4	4.2	220 ± 3	6.2 ± 0.7
10	3.9	200 ± 5	5.1 ± 0.7	3.9	185 ± 3	6.8 ± 1.1
11	3.9	223 ± 3	4.6 ± 0.6	3.8	199 ± 3	8.8 ± 1.2
12	4.4	172 ± 4	3.5 ± 0.5	4.4	147 ± 3	6.0 ± 0.8
13	3.6	205 ± 4	6.7 ± 0.8	3.5	190 ± 4	13.8 ± 2.0
14	5.0	217 ± 4	5.5 ± 0.7	5.0	189 ± 5	9.0 ± 1.3
15	4.4	225 ± 3	2.6 ± 0.3	4.3	206 ± 3	5.0 ± 0.6
16	4.8	213 ± 5	4.1 ± 0.6	4.7	190 ± 4	9.6 ± 1.5
Mean ± SD		210 ± 30	4.4 ± 1.4		190 ± 30	7.6 ± 2.3

data showed a good agreement with the clamped beam model, which is based purely on tensile deformation [25].

It is interesting to note that for fiber samples used in the fiber stability study (4 h at 135 °C and shown in Fig. 4), we did not observe any statistically significant change in diameter for 250 randomly selected fibers pre- and post-annealing (Fig. 6). Although the same fiber samples were used for these measurements, the regions selected within the sample were not the same pre- and post-annealing. The random variation in fiber size leads to virtually identical average diameters (250 ± 50 nm vs. 270 ± 50 nm). On the other hand, for the fibers used to determine the elastic modulus, the diameter of each of the 16 fibers was measured and compared both before and after treatment. This allows the heat treatment effect on diameter of each fiber to be determined directly which would not have been possible otherwise.

Effect of annealing treatment on crystallinity

Figure 9 shows the XRD spectra of as-spun PVA fibers and the fibers treated under the four different annealing conditions. The peak at $2\theta = 22.8°$ shows a gradual decrease in the FWHM as the annealing temperature increases. This is an indication of an increase in the crystallinity of PVA fibers. From Eq. 1, we determine that the crystallite size of as-spun PVA fibers increases from 3.5 to 5.2 nm after annealing for 4 h at 85 °C, and increases to 6.9 nm as the annealing temperature is elevated to 160 °C. The degree of crystallinity (X_c) of the fibers is 62 ± 1% after annealing for 4 h at 85 °C. The crystallinity of the fibers increases as the annealing temperature is increased and reaches a value of 81 ± 1% at an annealing temperature of 160 °C.

XRD spectra were obtained again after the annealed fibers were immersed in DI water for 1 day. The values of crystallite size and X_c are determined and are listed in Table 2. After the amorphous region of the 85 and 110 °C treated fibers are dissolved in DI water, the fibers are expected to have a higher degree of crystallinity. We observed a significant increase in the crystallinity of fibers treated at 85 and 110 °C after immersed in DI water for 1 day, with the increase being larger at 85 °C. The

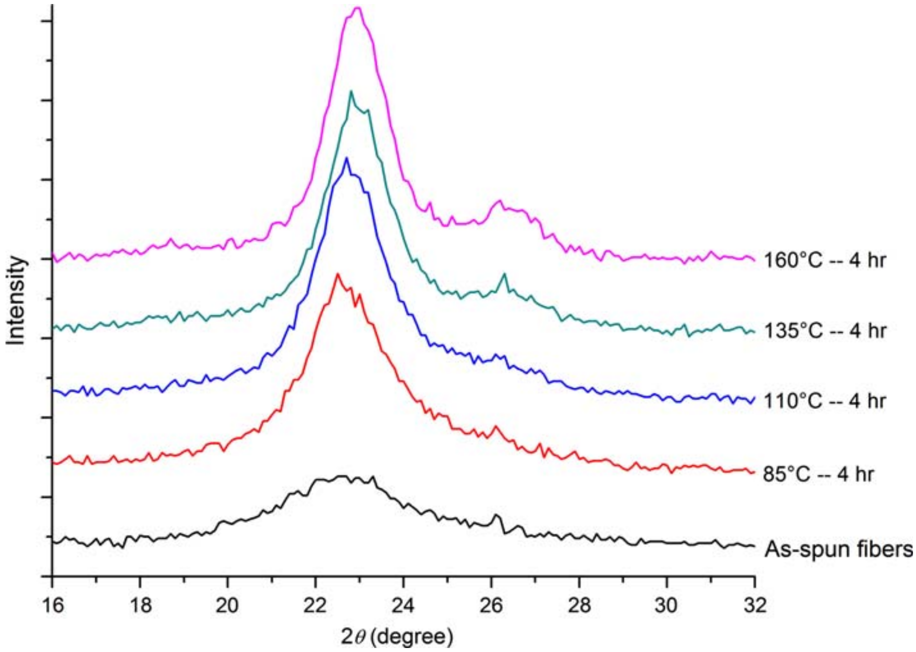

Fig. 9 XRD spectra (in the range between $2\theta = 16–32°$) of PVA as-spun fibers, and fibers after 4 h of four different annealing temperatures (arbitrary scale on intensity and offset for clarity)

Table 2 XRD results and mass loss of annealed PVA fibers before and after immersed in DI water for 1 day

Sample ($n = 3$)	Before immersed in DI water		After immersion in DI water for 1 day		
	Crystallite size (nm)	X_c (%)	Crystallite size (nm)	X_c (%)	Mass loss (%)
As-spun fibers	3.5 ± 0.1	57 ± 3	–	–	–
85 °C–4 h	5.2 ± 0.1	62 ± 1	4.2 ± 0.1	71 ± 2	67
110 °C–4 h	6.2 ± 0.1	68 ± 4	4.5 ± 0.1	72 ± 1	50
135 °C–4 h	6.6 ± 0.1	74 ± 2	4.6 ± 0.1	75 ± 1	0
160 °C–4 h	6.9 ± 0.1	81 ± 1	6.4 ± 0.2	83 ± 1	0

corresponding mass loss of the fiber mats are also reported in Table 2. The mass losses related to the dissolved amorphous region of the 85 and 110 °C treated fiber mats were measured at a value of 67 and 50%, respectively. For fibers annealed at 135 and 160 °C, the values of X_c and mass before and after immersed in DI water remain unchanged as the fibers are fully insoluble in the aqueous medium.

The effect of annealing treatment on the crystallinity of PVA is further quantified using an infrared spectroscopic method outlined by Kennedy et al. [29] and Peppas [30]. In Fig. 10, the intensity of the 1141 cm^{-1} band, which is associated with the symmetric C–C stretching mode, is shown to be sensitive to the degree of the crystallinity of PVA. Further, the FTIR spectra of the electrospun PVA fibers show that the intensity of the 1141 cm^{-1} band of the PVA fibers increases as annealing temperature increases. On the other hand, the intensity and shape of the 1425 cm^{-1} band, characteristic of $-CH_2-$ bonds, and the 1093 cm^{-1} band, characteristic of –CO– bonds, remain unchanged as a function of annealing temperature. These three bands are used to determine the vertical distances *a* and *b* as illustrated for the spectrum at 85 °C in Fig. 10. The ratio *a*/*b* is a measure of the relative increase in the crystallinity of the PVA fibers due to annealing treatment.

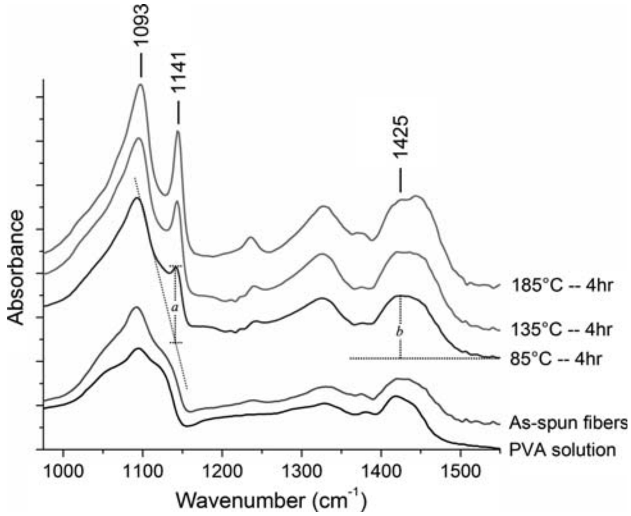

Fig. 10 FTIR spectra (in the range between 975 and 1550 cm^{-1}) of PVA solution, as-spun fibers, and fibers after 4 h of 85 °C annealing, 4 h of 135 °C annealing and 4 h of 185 °C annealing (arbitrary scale on absorbance intensity and offset for clarity)

Table 3 summarizes the data in this system. It includes the X_c in the XRD spectra and the ratio of *a*/*b* in the FTIR spectra obtained for PVA fiber samples ($n = 3$) after annealing treatment under the specified conditions. The results show the expected increase in the crystallinity of PVA from aqueous PVA solution to the as-spun fibers. Further, at a constant treatment time of 4 h, there is a systematic increase in fiber crystallinity with increasing annealing temperature up to 185 °C. The decrease of the *a*/*b* ratio at 210 °C is mostly likely due to its proximity to the melting transition temperature of PVA as determined by differential scanning calorimetry. At a constant annealing temperature of 110 °C, an increase in duration from 4 to 8 h led to a significant increase in crystallinity. On the other hand, at 135 °C, there is no change in crystallinity between 1 and 4 h of annealing. Based on these results, a criterion for aqueous stability of electrospun PVA fiber by annealing can be defined in terms of the *a*/*b* ratio in the FTIR spectra. A value of ~2.5 sets the boundary of fiber stability. With the *a*/*b* ratio ≥2.5, the fibers become stable. Similarly, the boundary of fiber stability can also be defined using the degree of crystallinity from XRD spectra, which is ~75% and above as shown in Table 3. These criterions can be used to determine the combination of treatment parameters, such as temperature and duration, to attain aqueous stability.

Table 3 Effect of annealing treatment on the crystallinity of electrospun PVA fibers

State	Annealing temperature (°C)	Duration (h)	Ratio of *a*/*b* in FTIR spectrum ($n = 3$)	X_c from XRD (%) ($n = 3$)	Fiber stability
PVA solution	–	–	0.09 ± 0.04	–	–
As-spun fibers	–	–	0.47 ± 0.05	57 ± 3	No
Fibers	85	4	1.63 ± 0.08	62 ± 1	No
	110	4	1.86 ± 0.02	68 ± 4	No
	110	8	2.16 ± 0.08	–	No
	135	0.5	2.16 ± 0.10	–	No
	135	1	2.49 ± 0.02	–	Yes
	135	4	2.46 ± 0.09	74 ± 2	Yes
	135	8	2.73 ± 0.11	–	Yes
	160	4	2.89 ± 0.10	81 ± 1	Yes
	185	4	3.10 ± 0.08	–	Yes
	210	4	2.88 ± 0.05	–	Yes

The increase in crystallinity though annealing also accounts for the increase in fiber stiffness, which is comparable to our previous study on PVA hydrogel. Low-temperature processing of the aqueous PVA solution results in solid hydrogels. Repeated thermal cycling then leads to an increase in crystallinity and in the elastic modulus of the hydrogel [26, 27]. The increase in elastic modulus of 80% after annealing at 135 °C for 4 h is significant. Based on the results shown in Table 3, the fiber stiffness can be controlled by a combination of changing treatment temperature and duration.

Conclusions

We developed a simple procedure to make use of controlled annealing as a post-processing treatment to improve the elastic modulus as well as the aqueous stability of electrospun PVA fibers.

We determined that both the aqueous stability and elastic modulus of electrospun PVA fibers increases with their crystallinity. After annealing for 4 h at 135 °C, we observed an 80% increase in the elastic modulus. Meanwhile, the fiber diameter decreased by 10%. FTIR and XRD showed that the treatment increased the crystallinity in the fibers as a function of annealing temperature and duration. The aqueous stability is defined by the ratio *a*/*b* of the FTIR band intensity at 1141 and 1425 cm^{-1}. A value of $a/b \geq 2.5$ in FTIR and $\sim$75% and above in crystallinity from XRD indicates fiber stability in water, which can be achieved by increasing the treatment temperature and/or treatment time. This information is useful for application of these fibers in an aqueous environment such as membrane filter and tissue scaffold.

Acknowledgements This work was supported by the Natural Sciences and Engineering Council of Canada (NSERC). We acknowledge technical assistance from Western Nanofabrication Facility, Dr. Jeffrey L. Hutter, Kimberley R. Law and Donna T. Padavan.

References

1. Formhals A (1940) US Patent 2187306
2. Li D, Xia Y (2004) Adv Mater 16:1151
3. Li M, Mondrinos MJ, Gandhi MR, Ko FK, Weiss AS, Lelkes PI (2005) Biomaterials 26:5999
4. Khil M-S, Cha D-I, Kim H-Y, Kim I-S, Bhattarai N (2003) J Biomed Mater Res 67B:675
5. Gopal R, Kaur S, Ma Z, Chan C, Ramakrishna S, Matsuura T (2006) J Membr Sci 281:581
6. Taepaiboon P, Rungsardthong U, Supaphol P (2006) Nanotechnology 17:2317
7. Xu CY, Inai R, Kotaki M, Ramakrishna S (2004) Biomaterials 25:877
8. Li W-J, Laurencin CT, Caterson EJ, Tuan RS, Ko FK (2002) J Biomed Mater Res 60:613
9. Stevens MM, George JH (2005) Science 310:1135
10. Li D, Wang Y, Xia Y (2004) Adv Mater 16:361
11. Zhang D, Chang J (2008) Nano Lett 8:3283
12. DeMerlis CC, Schoneker DR (2003) Food Chem Toxicol 41:319
13. Praptowidodo VS (2005) J Mol Struct 739:207
14. Carvalho LB, Araujo AM, Almeida AMP, Azevedo WM (1996) Sens Actuators B Chem 36:427
15. Rosiak JM, Ulanski P (1999) Radiat Phys chem 55:139
16. Rosiak JM (1994) J Controlled Release 31:9
17. Hassan CM, Peppas NA (2000) Biopolymers/Pva hydrogels/anionic polymerisation nanocomposites. Springer-Verlag Berlin, Berlin, p 37
18. Kobayashi M, Chang Y-S, Oka M (2005) Biomaterials 26:3243
19. Jiang H, Campbell G, Boughner D, Wan W-K, Quantz M (2004) Med Eng Phys 26:269
20. Zhou Y, Yang D, Chen X, Xu Q, Lu F, Nie J (2008) Biomacromolecules 9:349
21. Wang Y, Hsieh YL (2008) J Membr Sci 309:73
22. Yang D, Li Y, Nie J (2007) Carbohydr Polym 69:538
23. Yao L, Haas TW, Guiseppi-Elie A, Bowlin GL, Simpson DG, Wnek GE (2003) Chem Mater 15:1860
24. Naebe M, Lin T, Tian W, Dai L, Wang X (2007) Nanotechnology 18:225605
25. Wong KKH, Hutter JL, Zinke-Allmang M, Wan W (2009) Eur Polym J 45:1349
26. Millon LE, Mohammadi H, Wan WK (2006) J Biomed Mater Res B Appl Biomater 79B:305
27. Wan WK, Campbell G, Zhang ZF, Hui AJ, Boughner DR (2002) J Biomed Mater Res 63:854
28. Millon LE, Nieh MP, Hutter JL, Wan W (2007) Macromolecules 40:3655
29. Kenney JF, Willcockson GW (1966) J Polym Sci A-1 Polym Chem 4:679
30. Peppas NA (1977) Die Makromolekulare Chemie 178:595
31. Guhados G, Wan W, Hutter JL (2005) Langmuir 21:6642
32. Howard SA, Preston KD (1989) Rev Mineral Geochem 20:217
33. Fava R, Academic Press, New York (1980)
34. Hermans PH, Weidinger A (1961) Die Makromolekulare Chemie 44:24
35. Benedetti A, Cocco G, Fagherazzi G, Locardi B, Meriani S (1983) J Mater Sci 18:1039. doi:10.1007/BF00551972
36. Hutter JL, Bechhoefer J (1993) Rev Sci Instrum 64:1868